Quantum Well Electro-Optic Effects and Novel Device Applications

J. E. Zucker
AT&T Bell Laboratories
Holmdel, New Jersey 07733 USA

Received July 21, 1995

We demonstrate waveguide devices that employ unique semiconductor quantum well electrorefractive phenomena. Field- and carrier-induced changes in refractive index are applied to optical phase modulators, interferometric intensity modulators and balanced-bridge switches, directional coupler and digital optical switches. These quantum well devices are considerably more compact than the corresponding waveguide components made in bulk semiconductors, and require lower voltages. Moreover, one of the most important advantages to using quantum well material is the ability to customize the technology to system requirements. Through layer thicknesses, strain, composition, doping, and other material parameters, quantum well waveguide components can be tailor-made to meet specifications for polarization properties, loss, wavelength of operation, and other application-specific needs.

I. Introduction

Waveguide electro-optic devices are now being used in diverse optical systems such as antenna remoting and control, long-haul terrestrial and submarine fiber-optic communications, cable television distribution, instrumentations, and vehicle guidance. Where space is at a premium or weight is an issue compactness is key. Minimizing waveguide device length is also a critical factor in reducing the production cost, especially when the integrated optic device is monolithically integrated with other components for increased functionality. In applications where high speed is important, compact devices also have the advantage since they have reduced parasitics. However, there are some basic material constraints on how compact we can make electro-optic devices.

Consider the interferometric modulator shown in Fig. 1. A voltage V applied across a region of width w produces a refractive index change Δn. The active length of a modulator operating at wavelength λ needs to be at least $L \sim \lambda/(2\Delta n)$ to get an optical phase change of 180° and hence complete extinction of light. Suppose $w = 1$ μm and we want to keep $V < 5$ V. Then in order to keep this device under 1 mm in length we need a refractive index change per applied field $\Delta n/E > 1 \times 10^{-10}$ m/V. The linear electro-optic effect in bulk semiconductors like InP yields only $\sim 25 \times 10^{-12}$ m/V[1]. Thus for voltage- controlled, ultra-compact devices some type of enhanced electrorefraction is necessary.

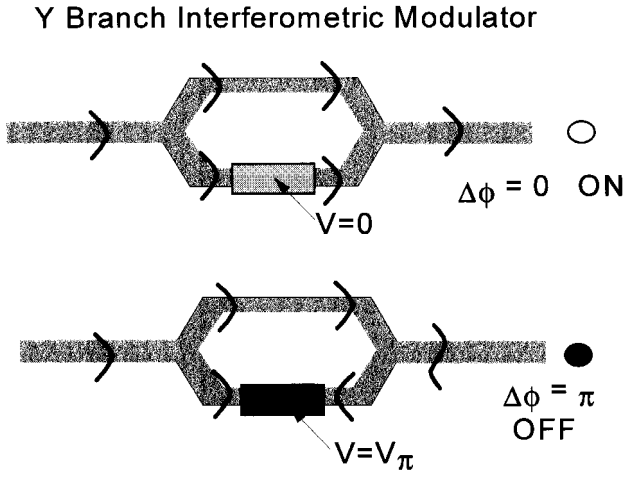

Figure 1: Top view of a Mach-Zehnder waveguide modulator. Constructive interference from both arms produces the "*ON*" state. A voltage-induced 180° optical phase change in one arm produces an antisymmetric mode that is not supported by the output waveguide and radiates into the substrate, producing the "OFF" state.

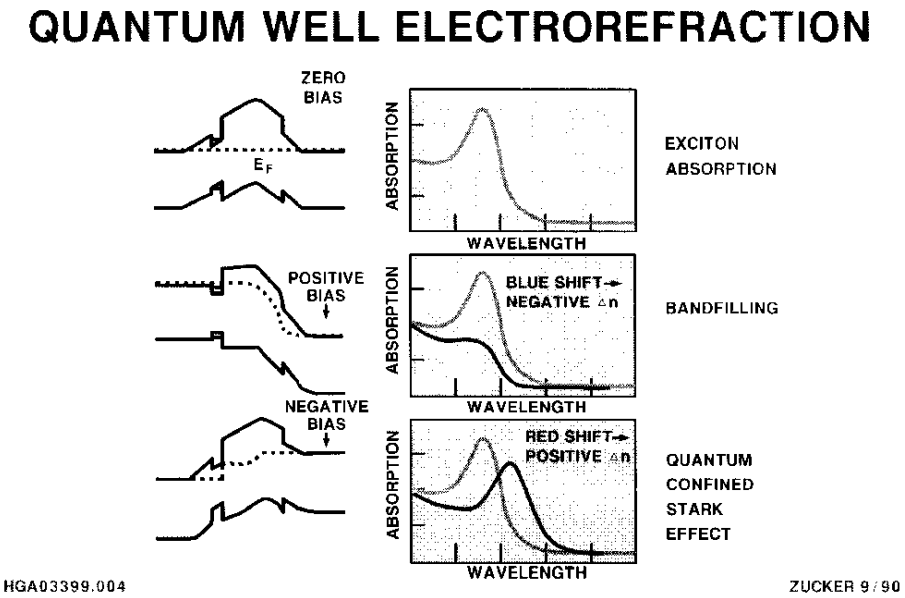

Figure 2: Spectral behavior of the absorption edge corresponding to near- bandedge electrooptic effects in quantum wells. On the left is the energy band diagram for a BRAQWET structure corresponding to zero- field (top), bandfilling (middle) and red-shifting of the exciton peak, or quantum confined Stark effect (bottom).

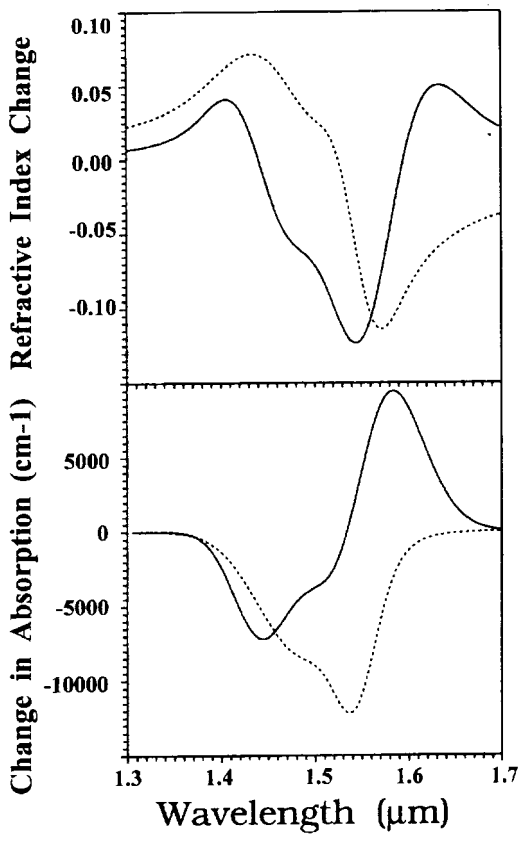

Figure 3: Voltage-induced changes in refractive index and absorption coefficient an InGaAs/InGaAlAs BRAQWET. The change in absorption coefficient refers to the thickness of the quantum well only.

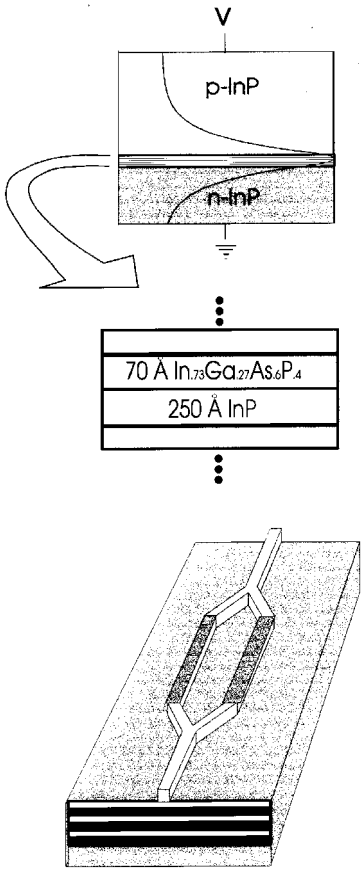

Figure 4: $P-i$(quantum well)-n waveguide cross- section is designed to place maximum optical mode intensity (solid line) at quantum wells. Mach-Zehnder modulator is formed by etching the uppermost $p-InP$ cladding layer to produce lateral confinement. Reverse bias to the $p-i-n$ produces Stark effect and index change in the active arms of the modulator.

In this paper we discuss novel electrorefractive phenomena in semiconductor quantum well waveguides that allow multi-gigahertz operation and, at the same time, provide low operating voltages and compact device lengths. These effects, associated with the quantum confined Stark effect (QCSE)[2] and phase space absorption quenching (PAQ)[3], can yield $\Delta n/E > 1 \times 10^{-9}$ m/V in quantum wells. We also describe some high-performance devices for modulation and switching that are based on such phenomena.

II. Stark Effect and Bandfilling in Quantum Wells

Fig. 2 illustrates two methods of inducing large refractive index changes in quantum wells. The bandstructure shown[4] contains, in addition to the quantum well, an electron reservoir n-doped layer and a p-doped barrier layer. At zero bias the BRAQWET (Barrier, Reservoir And Quantum Well Electron Transfer) structure has a small field across the quantum well. Nevertheless, electron and hole wavefunction overlap is still strong giving rise to a sharp excitonic absorption peak. When a positive bias is applied to the right-hand-side of the diagram, the field is reduced and electrons can flow into the well from the n-doped reservoir on the left. This causes a bleaching of the exciton absorption by bandfilling and a net blue shift of the absorption edge. The amount of refractive index change per carrier added to the quantum well in this way is essentially the same as for current-injection in bulk materials[5]. On the other hand, if negative bias is applied to the right-hand side, the field increases across the quantum well. This lowers the energy of the exciton transition and causes a red shift of the absorption edge.

Fig. 3 shows changes in absorption coefficient and refractive index that correspond to the above BRAQWET schematic. The sample consists of 70 Å InGaAs quantum well, 280 Å n-doped InGaAlAs reservoir layer (separated from the well by a 105 Å InGaAlAs undoped spacer), and on the other side, a 315 Å thick InAlAs barrier, of which 140 Å is p-doped. Dotted lines show changes in refraction and absorption for bandfilling with +5 V applied voltage, producing blue shift of the absorption edge, negative change in absorption coefficient, and negative index change at wavelengths below gap. Solid lines show changes in refraction and absorption for a -6 V applied voltage causing red-shift of the absorption edge, with positive increase in absorption and refractive index at wavelengths below gap.

Measurements of field-induced changes in refractive index have been made for a variety of quantum well systems including GaAs/AlGaAs[6], InGaAs/InP[7], and InGaAsP/InP[8]. For application to electrorefractive waveguide devices, where absorption and electroabsorption should be kept at a minimum, the quantum well crystal is generally grown with a zero-field bandgap 50-100 meV higher than the desired energy of operation. For example, in order to operate at 1.55 μm the ground state exciton transition should be designed (through choice of quantum well composition and thickness) to occur near 1.4 μm.

III. Mach-Zehnder Modulators

Extremely high data rate optical communications require external Mach-Zehnder intensity modulators for high-speed, adjustable-chirp modulation of optical signals. Other applications for Mach-Zehnder modulators include the distribution of cable television signals, antenna remoting, and instrumentation. One figure of merit for these modulators is $V \times L$, the product of the length and voltage needed to produce 180° phase shift and thereby switch the output from "on" to "off". In bulk InGaAsP, a low-switching-voltage InGaAsP waveguide interferometric modulator[9] was demonstrated with $V \times L = 22.5$ V- mm. Fig. 4 shows a schematic of the first quantum well waveguide interferometic modulator[10], formed from a strip-loaded p-i-n waveguide containing 10 undoped InGaAsP quantum wells surrounded by undoped InP buffer layers. With active length $L = 0.65$ mm, it required $V = 12$ V to switch. More recent p-i-n quantum well Mach- Zehnder modulators have dispensed with the undoped buffer layers and achieve voltage-length products $V \times L < 2$ V-mm[11]. High-speed versions[12] of the p-i(quantum well)-n Mach Zehnder modulator with reduced parasitic capacitance and thick quantum well regions have successfully operated at 10 gigabits per second. In addition, rib waveguide Mach-Zehnder modulators can be etched in an n-InAlAs/multiple BRAQWET/n-InAlAs waveguide. With eight repeated BRAQWETs as the electrooptically-active core, a $V \times L = 2.1$ V-mm (with

an active length Mach-Zehnder arm 0.7 mm in length) was demonstrated[13].

IV. Space-Division Switches

Many functions inside an optical network require routing of light from one spatial port to another. For example, protection switching is used to re-establish service with a backup set of fibers when a cable connection is cut. In time-multiplexed systems, space-switches are needed to pick-apart a high-data-rate optical bit-stream into lower-rate streams. Space switches are also used to dynamically reconfigure the optical interconnections between electronic modules, or to provide true-time-delay for radar beamforming. For small size, low voltage and high-speed, quantum well-based switching provides some advantages. The same p-i(multiple quantum well)-n and n-(multiple BRAQWET)-n waveguide structures used for modulators can also be applied to space-division switches. Fig. 5 shows a diagram of the first quantum well directional coupler switch[14]. With a 450 μm-long coupling region, switching between cross-over and straight-through states was achieved with symmetric 8 dB extinction for an applied field 13 V/μm. On the other hand, the dashed line in Fig. 5 shows that even with a waveguide core completely filled with InGaAsP of the same bandgap, the required switching voltage would exceed the reverse breakdown voltage of the diode. More recently, the first 4 × 4 directional coupler switch matrix was demonstrated[15] using the Stark effect in a p-i (InGaAs/InGaAlAs quantum well)-n structure.

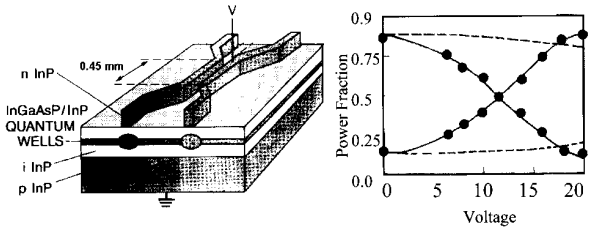

Figure 5: Directional coupler switch formed by etching the uppermost n-cladding from an n-i(quantum well)-p waveguide wafer containing 10 quantum wells inside the 1.49 μm thick i-region. For zero applied voltage, light couples over from one waveguide to the next. As reverse bias increases, the difference in refractive index destroys coupling between the two waveguides and light exits the straight - through port. At right, the measured fraction of output power in cross-over and straight-through ports is plotted (dots) as a function of applied voltage. The dashed line gives the switching curve to be expected if the entire i-region contained bulk InGaAsP instead of InGaAsP quantum wells.

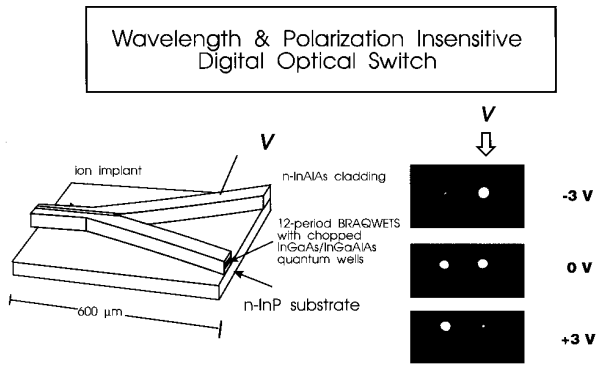

Figure 6: Digital optical switch formed from BRAQWET waveguide and pictures of the near- field output intensity from the two branches. At 0 V, the device is a 50:50 3 v splitter. For -3 V applied, the Stark effect produces a positive refractive index change, drawing light to exit the biased port. For +3 V, bandfilling depresses the refractive index causing light to exit the unbiased side.

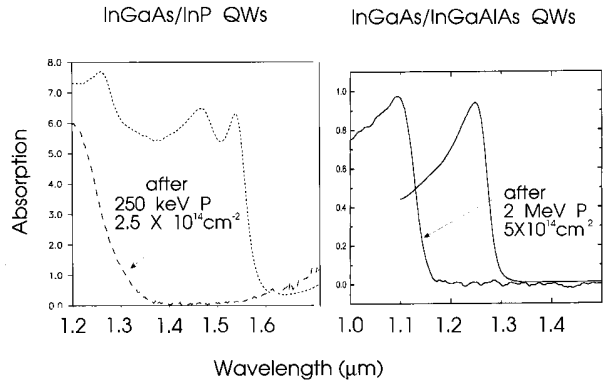

Figure 7: Intermixing of quantum wells via ion implantation to reduce propagation loss. The energy of the P implant determines the position of peak damage in the layers; the dose shown is the maximum it can be before destroying electrical properties of the p-i-n junctions. The large blue-shifting of the bandedge results in a large reduction in propagation loss at below-gap wavelengths.

Fig. 6 shows a 1 × 2 Y-branch switch based on the BRAQWET structure[16]. It is termed a digital switch for the digital-like switching characteristic which is not periodic in the voltage (as in a directional coupler). Light is drawn to the port with the higher refractive index and it does not flow back, making the digitial switch both polarization and wavelength insensitive[17]. Digital switches have also been made using p-i(quantum well)-n structures. In the BRAQWET digital switch, both positive and negative voltages can be applied to a single side of the switch (as in Fig. 6) to produce switching. Alternatively, both sides can be biased in push-pull

fashion to decrease the required voltage swing by a factor of two; e.g, +1.5 V to one side and -1.5 V to the other yields the same switch state as 3 V single-sided drive. In a p-i-n digital switch, push-pull switching requires a DC offset to maintain reverse bias conditions.

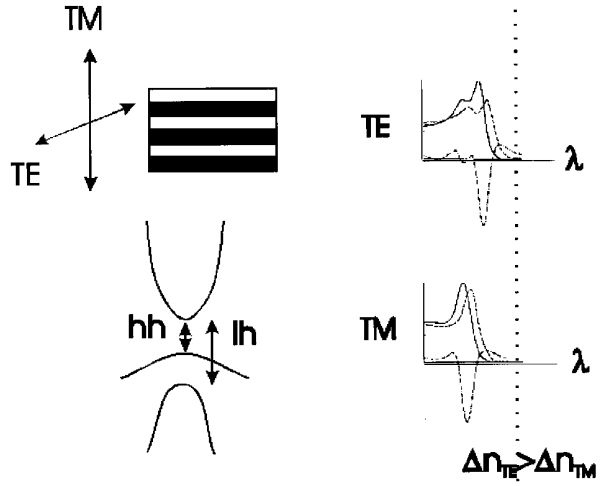

Figure 8: Polarization anisotropy in lattice-matched quantum wells. The periodic potential lifts the degeneracy between the heavy- and light-hole valence bands, causing two excitonic peaks associated with heavy hole(hh) and light hole(lh) to conduction band absorption. In the TE polarization (in the plane of the layers), both transitions participate. However in the TM polarization (perpendicular to the layers) only the light hole transition appears because of its symmetry. The refractive index change Δn at long wavelengths from near-bandedge electroabsorption is always larger for the TE polarization, since in lattice- matched quantum wells the hh transition is lower in energy.

For switches and especially large switch arrays, minimizing the propagation loss is always a priority. Fig. 7 shows a method that works for both BRAQWET and p-i-n switch material: quantum well intermixing via ion implantation. In areas of the photonic integrated circuit where shorter wavelength bandgap is needed, damage sites are created by the implanted ions (other parts are masked off during the implant by photoresist). During thermal anneal, wells and barriers are intermixed as defects migrate through the layers. A shorter wavelength bandgap characteristic of the equivalent random alloy is produced. The peak of the damage profile is accurately placed by choosing the ion energy. For intermixing MOCVD-grown InGaAs/InP wells, lower energy P implantation was followed by regrowth[18] of the InP:Zn cladding to avoid Zn diffusion. In MBE-grown InGaAs/InGaAlAs wells, where InGaAlAs:Be is the p-type upper cladding, implantation at 2 MeV was done with the cladding layers in place[19]. Both methods result in a large blue-shift of the bandedge,as shown in Fig. 7, and a significant reduction in waveguide loss. Moreover, p-i-n junction characteristics are maintained after implant, permitting electrical isolation between blue-shifted and non-shifted regions of a circuit. The P-implant technique has also produced buried quantum well heterostructure waveguides without any regrowths[20], since blue-shifting of the bandgap also results in a reduction in quantum well refractive index. In addition, the P-implant technique has been successfully demonstrated as a means for loss reduction in BRAQWET waveguides[21].

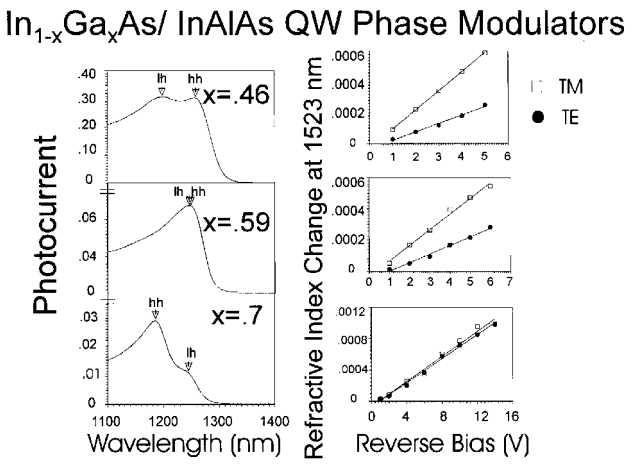

Figure 9: Left: photocurrent spectra of InGaAs/InAlAs quantum wells as a function of increasing tensile strain. By increasing a content, tensile strain is increased to place the light hole valence band closer to the heavy hole valence band (center). For extreme tension, the light hole exciton peak (lh) is actually lower in energy than the heavy hole (hh) exciton peak (bottom). At right, the measured refractive index change as a function of voltage shows that as tensile strain is increased, the ratio of refractive index change in the TM polarization to that in the TE polatization is increased.

One of the results of quantum confinement is a lifting of the degeneracy between light- and heavy-hole valence bands.This creates a severe polarization

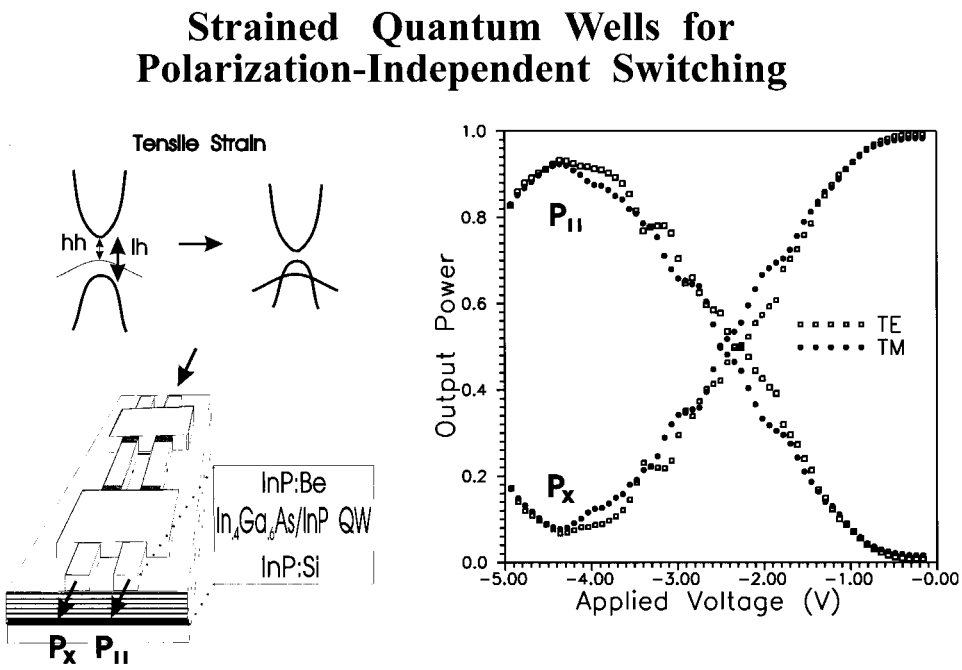

Figure 10: A polarization- independent balanced bridge switch is made by using tensile-strained quantum wells as the electro-optically active waveguide core. The switching characteristics at right show nearly identical behavior for TE and TM polarizations. At 0 V, straight-through state has < -17 dB crosstalk in both polarizations; at -4.5 V, the crossover state has < -10 dB crosstalk in both polarizations. The voltage- length product for the switch is 3.0 V-mm.

anisotropy for quantum well waveguide devices and is a drawback for quantum well switches in systems where the incoming polarization is random. In unstrained quantum wells, as shown in Fig. 8, electrorefraction at some below-gap wavelength λ_{op} is larger for TE than for TM polarization because of the greater proximity of the heavy-hole exciton peak at λ_{hh}. However, the ordering of valence bands can be reversed by growing the well with built-in tensile strain. The concept is explicitly demonstrated in Fig. 9, where we show the effects of increasing tensile strain on MBE-grown InGaAs/InGaAlAs QW phase modulators[22]. In the near-lattice-matched case (Ga fraction x=.46 in the InGaAs well) we have $\lambda_{hh} > \lambda_{lh}$ and the phase shift efficiency in the TE polarization is 2.4 times that in the TM. For x=.59, $\lambda_{hh} \sim \lambda_{lh}$ but owing to the difference in oscillator strength of the two transitions polarization-independence is not yet acheived. Equal TE and TM index change at 1.5 μm is obtained only at higher tensile strain,when x=0.7. The same concept using tensile wells has recently been used to produce the first polarization-independent quantum well waveguide switch in CBE-grown $In_{.4}Ga_{.6}As/InP$ material[23] as shown in Fig. 10.

Monolithic integration

One of the attractive features of semiconductor switches and modulators is the ability to monolithically integrate other components for increased functionality. Quantum well waveguide devices can be integrated with electronic as well as photonic components as shown in Figs. 11 and 12. In the optoelectronic circuit for wavelength conversion[24], quantum well p-i-n waveguides are used as photodetectors for incoming modulated input and as modulators for transferring the signal onto a second wavelength. Photocurrent from the input waveguide goes to a three stage heterojunction bipolar transistor (HBT) transimpedance amplifier. The base wafer is created in a single growth, with the p-i(quantum well)-n followed by the HBT layers. A series of stop-etch layers precisely defines the depth of each feature. For the integrated laser/Mach-Zehnder modulator[25] shown in Fig. 12, the base wafer again contains all the critical layers in the same growth. The electrorefractive quantum wells are grown first with bandgap near 1400 nm to produce index change at 1550 nm, followed by the gain quantum wells with bandgap of 1550 nm. After etching the waveguide geometry and definition of the DBR grating, the wafer undergoes two

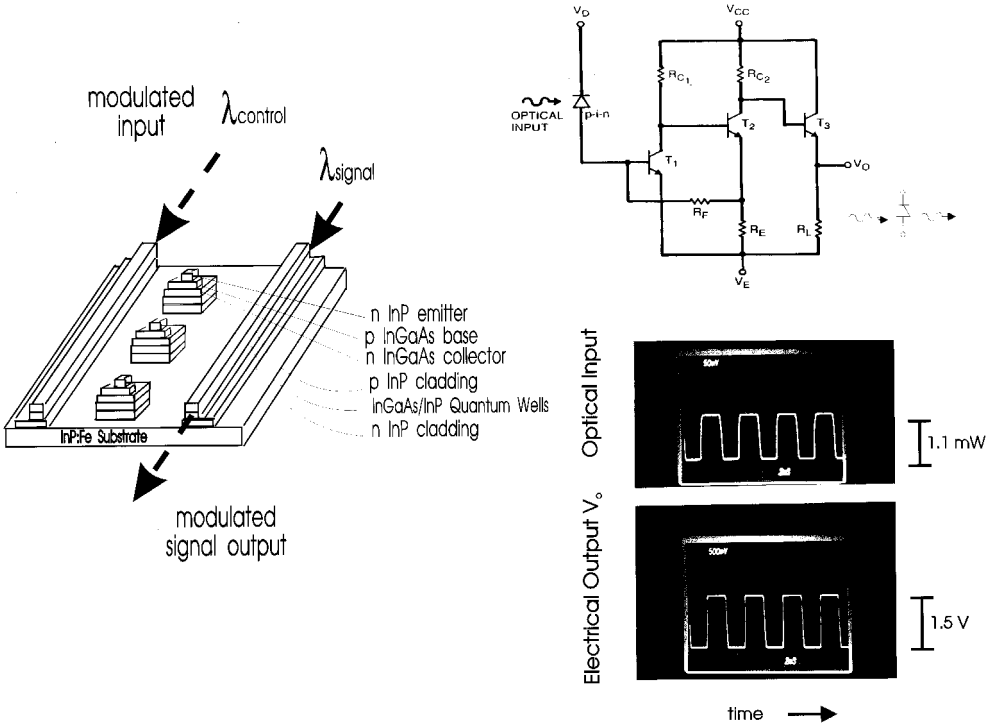

Figure 11: Monolithicallly integrated p-i(quantum well)-n waveguide photodetectors and modulators with heterojunction bipolar transistor circuit form an optoelectronic circuit for wavelength conversion. At left, the structure of the wafer. P-i(quantum well)-n layers are formed into waveguides; transistor layers are etched to form the circuit in the center. At upper right is the circuit diagram of the transimpedance amplifier transistor circuit which collects photocurrent signal from the input waveguide photodiode. The circuit creates an output voltage to drive the second waveguide modulator with a replica of the optical input. At lower right are the oscilloscope traces showing optical input (1.1 mW in magnitude) and electrical output of the circuit, 1.5 V, which is sufficient to drive the modulator waveguide output stage.

regrowths: semi-insulating InP for blocking and p-InP for the upper contact. The reverse-biased modulator section and the forward-biased gain section are electrically isolated via proton implantation.

References

1. K. Tada and N. Suzuki, Jpn. J. Appl. Phys. **19**, 2295 (1980).
2. D. A. B. Miller, D. S. Chemla, T. C. Damen, A. C. Gossard, W. Wiegmann, T. H. Wood, and C. A. Burrus, Phys. Rev. B **32**, 1043 (1985).
3. D. S. Chemla, I. Bar-Joseph, C. Klingshirn, D. A. B. Miller, J. M. Kuo and T. Chang, Appl. Phys. Lett. **50**, 585 (1987).
4. M. Wegener, J. E. Zucker, T. Y. Chang, N. J. Sauer, K. L. Jones, D. S. Chemla, Phys. Rev. B,**41**, 3097 (1990).
5. J. E. Zucker, T. Y. Chang, M. Wegener, N. J. Sauer, K. L. Jones, D. S. Chemla, Photonics Technol. Lett. **2**, 29 (1990).
6. J. E. Zucker, T. L. Hendrickson and C. A. Burrus, Appl. Phys. Lett. **52**, 945 (1988).
7. J. E. Zucker, I. Bar-Joseph, G. Sucha, U. Koren, B. I. Miller, D. S. Chemla, Electron. Lett. **24**, 458 (1988).
8. J. E. Zucker, I. Bar-Joseph, B. I. Miller, U. Koren, and D. S. Chemla, Appl. Phys. Lett. **54**, 10 (1989).
9. H. Takeuchi, K. Kasaya, and K. Oe, IEEE Photonics Technol. Lett.**1**, 227 (1989).
10. J. E. Zucker, K. L. Jones, B. I. Miller, and U. Koren, Photon. Technol. Lett. **2**, 32 (1990).
11. J. E. Zucker, K. L. Jones, B. I. Miller, M. G. Young, U. Koren, J. D. Evankow and C. A. Burrus, Appl. Phys. Lett. **60**, 277 (1992).
12. C. Rolland, R. S. Moore, F. Shepherd, and G. Hillier, Electronics. Lett. **29**, 471 (1993); H. Sano,

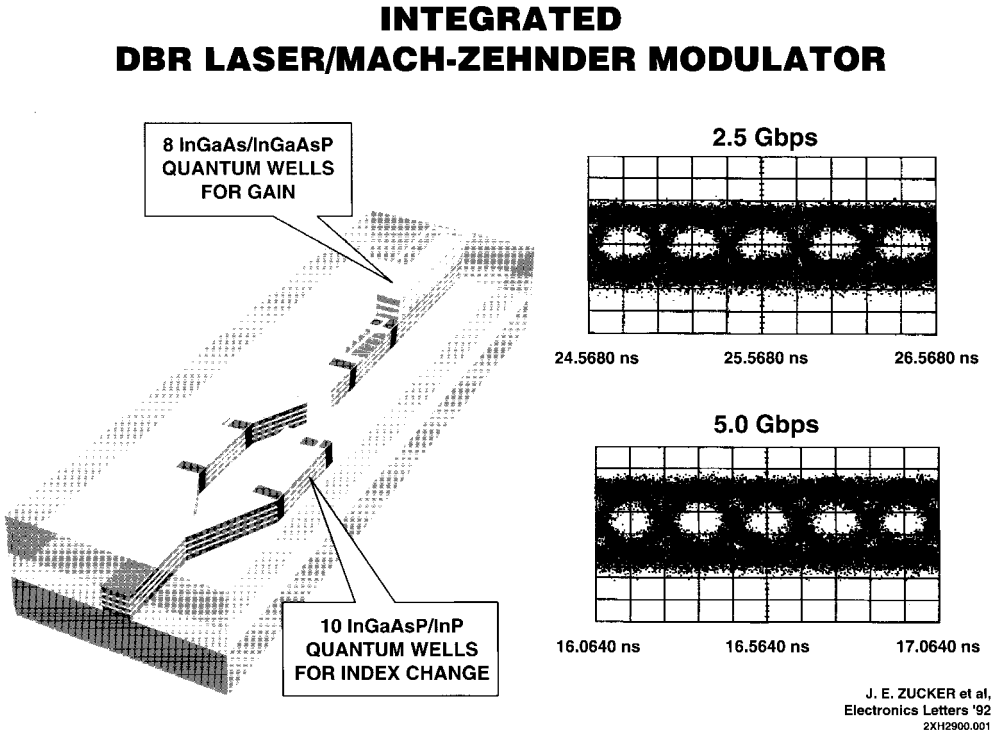

Figure 12: Integrated DBR laser/Mach-Zehnder modulator is wavelength-tunable about 1550 nm, transmits at 2.5 and 5. 0 gigabits per second, and has total length 1.74 mm, including 0. 67 mm for gain, 0.23 mm for Bragg reflector grating region, and Mach-Zehnder with 0.4 mm active length. It uses two sets of quantum wells, the lower one for index modulation (with bandgap near 1400 nm) and the upper one for gain at 1550 nm. In the modulator region, the gain quantum wells are etched off before the etching of the waveguide pattern and final regrowths.

T. Ido, S. Tanaka, H. Tsushima and A. Takai, "High speed properties of InGaAs/InAlAs MQW Mach-Zehnder modulators," Proc. IEICE Spring Meeting, p.4-187 (1993).

13. J. E. Zucker, K. L. Jones, T. Y. Chang, N. Sauer, B. Tell, M. Wegener and D. S. Chemla, Electron. Lett. **26**, 2030 (1990).
14. J. E. Zucker, K. L. Jones, M. G. Young, B.I. Miller, U. Koren, Appl. Phys. Lett. **55**, 2280 (1989).
15. H. Takeuchi, Y. Hasumi, S. Kondo, Y. Noguchi, Electron. Lett. **29**, 523 (1993).
16. Y. Chen, J. E. Zucker, T. Y. Chang, N. J. Sauer, B. Tell, "Y-branch electrooptic waveguide switch at 1.55 μm using chopped quantum well electron transfer structure," Integrated Photonics Research Technical Digest, 1993 (Optical Society of America, Wash. DC) pp.176-179.
17. M. N. Khan, J. E. Zucker, T. Y. Chang, N. J. Sauer, M. D. Divino, Photon. Technol. Lett. **3**, 394 (1994).
18. J. E. Zucker, B. Tell, K. L. Jones, M. D. Divino, K. Brown-Goebeler, C. H. Joyner, B. I. Miller, and M. G. Young, Appl. Phys. Lett. **60**, 3036 (1992).
19. Y. Chen, J. E. Zucker, B. Tell, N. J. Sauer and T. Y. Chang, Electron. Lett. **29**, 87 (1993).
20. J. E. Zucker, K. L. Jones, B. Tell, K. Brown-Goebeler, C. H. Joyner, B. I. Miller and M. G. Young, Electron. Lett. **28**, 853 (1992).
21. J. E. Zucker, M. D. Divino, T. Y. Chang and N. J. Sauer, Photon. Technol. Lett. **6**, 1105 (1994).
22. Y. Chen, J. E. Zucker, N. J. Sauer, T. Y. Chang, Photon. Technol. Lett. **4**, 1120 (1992).
23. J. E. Zucker, K. L. Jones, T. H. Chiu, B. Tell, J. Lightwave Technol. **10**, 1926 (1992).
24. J. E. Zucker, Y. Chen, M. D. Divino, S. Chandrasekhar, C. H. Joyner and C. A. Burrus, "Monolithic integration of quantum well optical waveguides with heterojunction bipolar electronics for

wavelength switching," in *Photonics in Switching Technical Digest.* 1993 (Optical Society of America, Wash. DC) pp.29-32.

25. J. E. Zucker, K. L. Jones, M. A. Newkirk, R. P; Gnall, B. I. Miller, M. G. Young, U. Koren, C. A. Burrus, B. Tell, Electron. Lett. **28**, 1888 (1992); J. Lightwave Technol. **10**, 924 (1992).